forests

Article

Soil Erosion Risk Analysis in the Ría de Arosa (Pontevedra, Spain) Using the RUSLE and GIS Techniques

Carlos E. Nieto [1,*], Antonio Miguel Martínez-Graña [1] and Leticia Merchán [2]

[1] Department of Geology, Faculty of Sciences, Merced Square, University of Salamanca, 37008 Salamanca, Spain; amgranna@usal.es
[2] Department of Soil Sciences, Faculty of Agricultural and Environmental Sciences, University of Salamanca, Filiberto Villalobos Avenue, 119, 37007 Salamanca, Spain; leticiamerchan@usal.es
* Correspondence: carlosenriquenm@usal.es

Abstract: Soil erosion in coastal areas, driven by global change and human activity, poses a significant threat to ecological and economic stability. This research investigates water erosion in the southeast of the Ría de Arosa (Pontevedra, Spain), utilizing the Revised Universal Soil Loss Equation model and Geographic Information System technologies. Key factors analyzed include rainfall erosivity, soil erodibility, topography, land cover, and conservation practices. High-resolution maps (1 × 1 m pixels) identified areas at high risk of erosion. Vulnerable zones, such as coastal cliffs and vineyards, show severe erosion rates exceeding 50 t/ha/year (>5 mm/year), with the most extreme zones reaching up to 200 t/ha/year (>200 mm/year). These results emphasize that intervention could be required or recommended. Suggested measures include reforestation, effective agricultural land management, or the implementation of vegetative barriers to reduce erosion. These areas, characterized by steep slopes and sparse vegetation, are particularly susceptible to soil loss, necessitating specific conservation efforts. The results underscore the need for sustainable coastal management practices and preventive strategies to protect this vulnerable coastal zone. Implementing these measures is crucial to mitigating the impacts of soil erosion, preserving natural resources, and ensuring long-term ecological and economic resilience in the region.

Keywords: soil erosion; erosion risk; RUSLE; GIS; coastal management

check for updates

Citation: Nieto, C.E.; Martínez-Graña, A.M.; Merchán, L. Soil Erosion Risk Analysis in the Ría de Arosa (Pontevedra, Spain) Using the RUSLE and GIS Techniques. *Forests* **2024**, *15*, 1481. https://doi.org/10.3390/f15091481

Academic Editors: Hongwei Xu, Jun Xiao and Danbo Pang

Received: 12 July 2024
Revised: 14 August 2024
Accepted: 21 August 2024
Published: 23 August 2024

Copyright: © 2024 by the authors. Licensee MDPI, Basel, Switzerland. This article is an open access article distributed under the terms and conditions of the Creative Commons Attribution (CC BY) license (https://creativecommons.org/licenses/by/4.0/).

1. Introduction

Coastal areas around the planet represent regions of special ecological value [1]. They host unique biomes, climates, and geomorphological features [2]. Additionally, they are ideal locations for the economic and recreational development of human activities [3,4]. Currently, these areas are home to approximately 896 million people, accounting for about 11% of the global population in 2020 [5]. This entire population is exposed to problems associated with global change along coastlines [5]. Rising sea levels, subsidence, and increasingly frequent storms necessitate the development of land management and production strategies for soil conservation [6–8]. Issues associated with anthropogenic productive or tourist activities lead to ecosystem degradation, which, along with the previously mentioned factors, highlight the high vulnerability of the entire environment [9,10].

Soil erosion is one of the main problems humanity faces in the 21st century [11]. Soil loss directly affects the maintenance of natural resources and agricultural production, influencing food security and water availability [12–14]. Agricultural and livestock activities directly rely on the soil's productive capacity, accounting for 95% of the world's food production [11]. Additionally, soils are important reservoirs of organic matter, and their loss directly impacts the carbon cycle and Soil Organic Carbon (SOC) dynamics [15]. Urbanization resulting from rapid human development and population growth contributes significantly to soil erosion [9,10]. Similarly, poor management and changes in land use significantly increase the rates of water erosion [15–17].

Water erosion is the natural process generated by the combined action of the erosive capacity of raindrops, surface runoff flow, and the susceptibility of soil to being eroded. The direct erosion mechanisms combine the kinetic energy of raindrop impact on the substrate, causing soil disaggregation, with the flow's action as a transport agent. Other factors, such as slope gradients or the development of rills and gullies, amplify the process's effectiveness [18–20]. There are different empirical techniques for estimating water erosion rates: Universal Soil Loss Equation (USLE), Soil and Water Assessment Tool (SWAT), Water Erosion Prediction Project (WEPP), etc. [21–26]. This work presents a study of water erosion in the southeast of the Ría de Arosa based on the Revised Universal Soil Loss Equation (RUSLE) [27,28], using GIS techniques with ArcGIS 10.8©. This methodology has been successfully applied in other innovative water erosion calculation studies [29–32]. The RUSLE water erosion model involves the analysis of five factors: rainfall erosivity (R-Factor), soil erodibility (K-Factor), topographic factor (LS-Factor), land use cover factor (C-Factor), and conservation practices factor (P-Factor) [27,28]. It serves as a modeling tool that provides immediate, high-resolution results (1×1 m pixels in this study) and offers continuous monitoring, allowing rapid updates of results based on parameter variation.

Analyzing water erosion in coastal areas, such as the southeast of the Ría de Arosa, is crucial due to the fragility of these environments and the anthropogenic pressure they face. Identifying and quantifying the most vulnerable areas allows for the development of effective mitigation and conservation strategies. In recent years, Galicia has experienced a significant increase in the number of forest fires [33,34], which has heightened soil vulnerability to water erosion [35,36]. The main objective of this study is to apply the RUSLE methodology to determine water erosion rates in the region and propose corrective measures to minimize soil loss. The risks will be analyzed concerning different land uses and urban areas. The results obtained will provide a solid foundation for the sustainable management of natural resources in this coastal area, providing key information for decision-making and the implementation of conservation practices.

Study Area

This study focuses on the southeastern margin of the Ría de Arosa in the province of Pontevedra (Galicia, Spain) (Figure 1). The term "Ría" is used to describe an ancient coastal river valley flooded by the sea during the Quaternary period. The Ría de Arosa is the most important estuary of the Rías Bajas, located in the northwest of the Spanish coastline. The most prominent municipalities in the area are Villanueva de Arosa, Arosa, Cambados, El Grove, Portonovo, and Sanxenxo. These municipalities, along with other smaller populations, have a stable population of approximately 57,358 inhabitants in an area of 9600 hectares, resulting in a population density of 598 inhabitants per km^2, more than six times the national average (96 inhabitants per km^2) (data from the National Institute of Statistics (INE), https://www.ine.es/, accessed on 5 July 2024).

The climate of the area is temperate, with a dry and mild summer (Csb) [37]. The ocean's regulating effect favors mild average temperatures throughout the year, ranging from 19.3 °C in summer to 9 °C in winter. The average annual precipitation is 1455 mm (information provided by the State Meteorological Agency (AEMET), https://www.aemet.es/es/serviciosclimaticos/datosclimatologicos, accessed on 5 July 2024).

From a geological perspective, the area belongs to the northwestern section of the Iberian Massif. It is an internal zone of the Variscan Orogen, where allochthonous domains (schists and paragneisses of the Malpica Tui Unit) are in contact with the autochthonous Paleozoic metasediments of the Central Iberian Zone and early and late variscan granites [38]. The relief is influenced by various geomorphological units, showing the steepest slopes in areas with granitic domes and in summits, ridges, and hills belonging to lithostructural morphogenetic systems [39,40]. The coastal influence generates numerous coastal units, such as beaches, dune systems, tombolos, and marine terraces. Additionally, the tidal coastal dynamics favor the development of marshes. Therefore, two protected natural areas have been established by the Natura 2000 Network: the Umia–O Grove Intertidal Complex and the Ons–O Grove Complex.

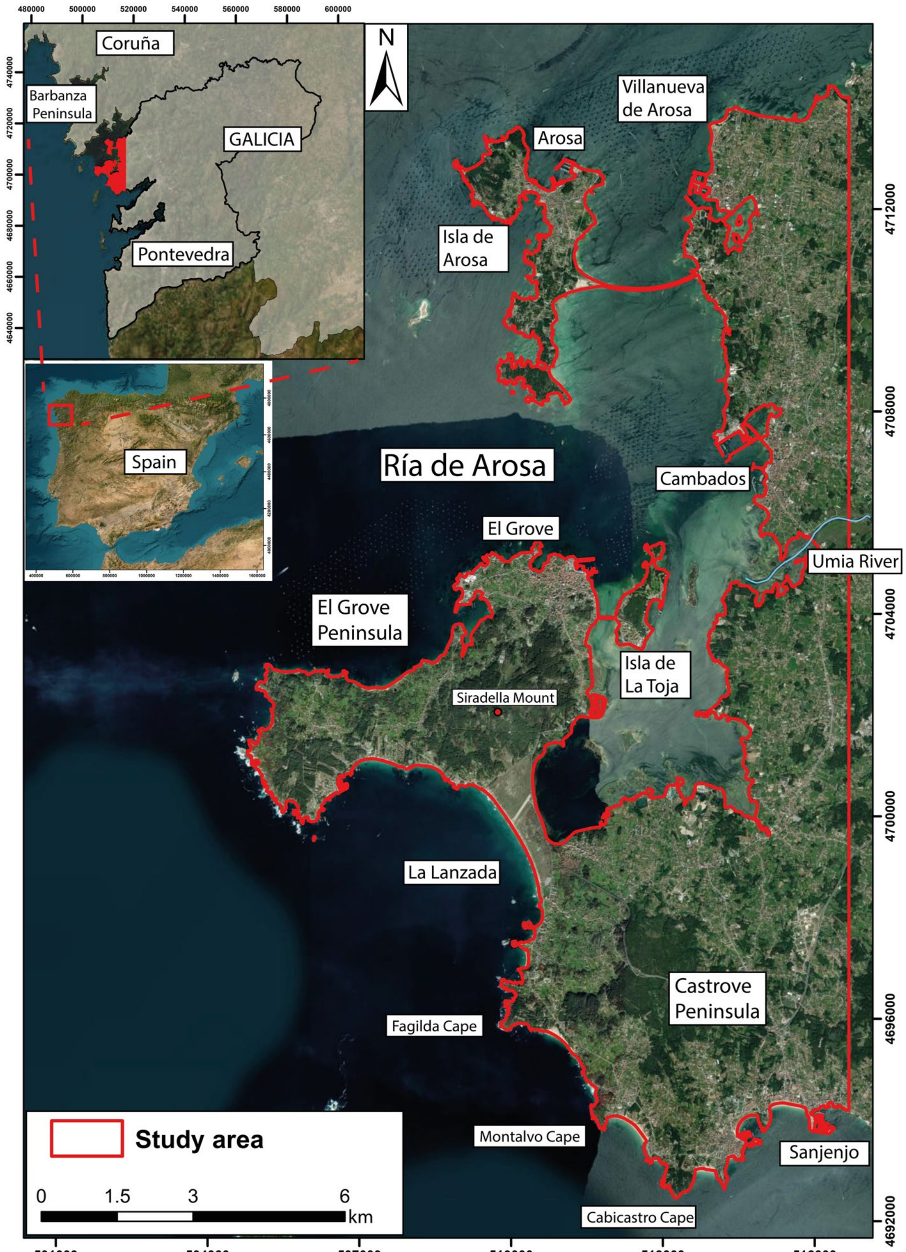

Figure 1. Location map of the study area within the province of Pontevedra in Galicia.

The lithological characteristics and morphology of the relief influence the formation and development of different soil types in the territory. On slightly weathered granitic rocks, juvenile, poorly developed, very acidic soils with a high aluminum concentration (aluminum soils) are recognized [41,42]. These soils are favorable for the development of eucalyptus and pines, the main species of the area's forests [43]. The most common soil types are Leptosols and Umbrisols, although Cambisols and Regosols are also found more frequently. On metamorphic rocks (slates and schists), soils with properties and types like those described in granitic environments are found [41,42]. Finally, on recent Quaternary deposits, Arenosol (coastal sandy soils) and Fluvisol (alluvial or marshy deposits) soil types are distinguished [42].

2. Materials and Methods

In this study, both fieldwork and office work were combined to obtain and process the data. First, successive field campaigns were conducted to collect information primarily on the physical characteristics of the environment. Abiotic aspects (lithological, geomorphological, edaphic, topographical, etc.) and biotic aspects, such as vegetation characteristics in the study area, were analyzed. The field reconnaissance was complemented by the development of a comprehensive database that collects detailed and updated information (rainfall, forest, satellite data, etc.). The information is highly up-to-date and features high resolution through the creation of a raster with a pixel size of 1 × 1 m, increasing the value of the data presented here. Data processing was carried out using a Geographic Information System (GIS) (ArcGIS 10.8), where a series of maps with empirical data were obtained and used for calculating potential and actual erosion (Figure 2).

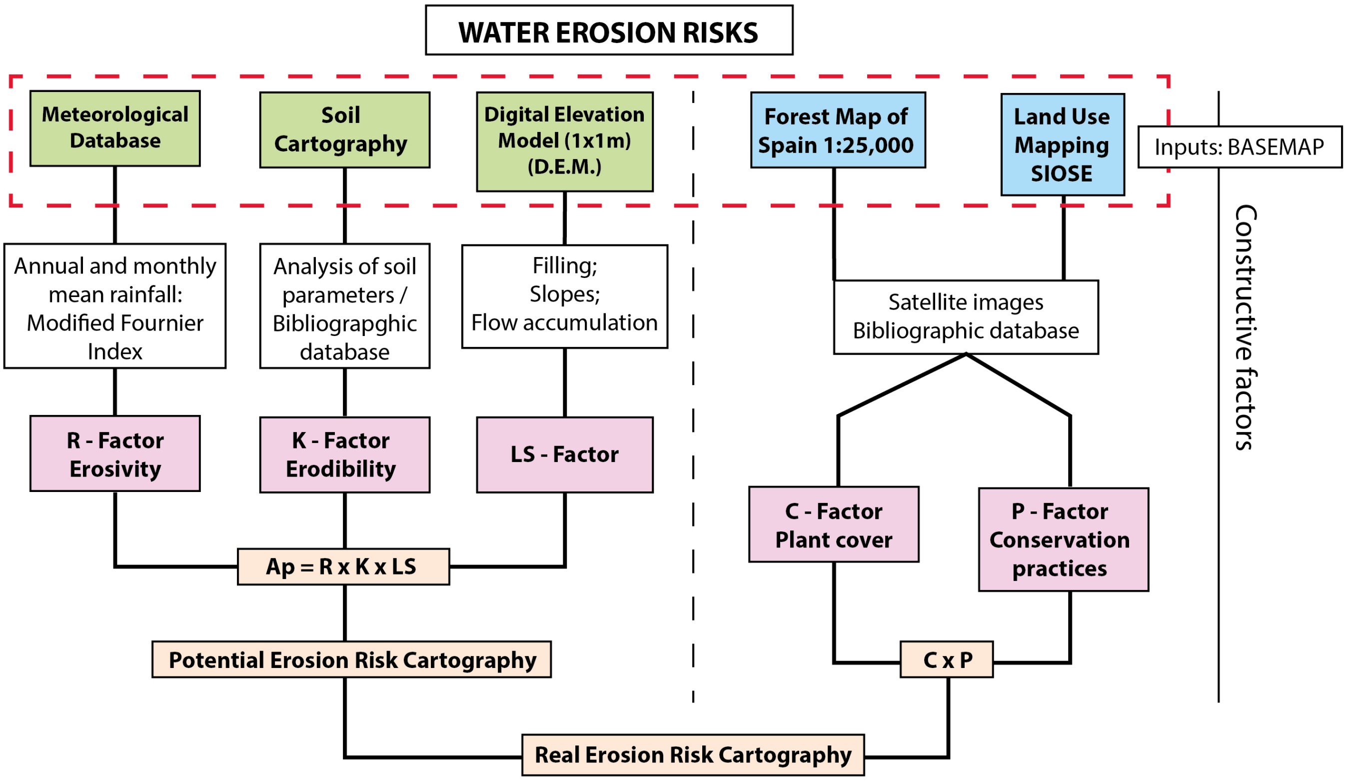

Figure 2. Methodological scheme.

2.1. Potential Erosion Mapping

In potential erosion mapping, the degree of susceptibility of an area to water erosion is evaluated. To achieve this, it is crucial to conduct a preliminary study of the physical factors that directly influence this process. The values involved in potential erosion combine information on precipitation, soil mechanical resistance, and terrain topography, considering both the length and slope of the inclines. This territorial analysis is conducted using the Revised Universal Soil Loss Equation (RUSLE) [27,28], adapting its different parameters according to the specific characteristics of the study area. The factors used in the calculation of potential erosion are erosivity (R-Factor), erodibility (K-Factor), and the LS-Factor (slope length and steepness), which are combined according to Equation (1):

$$Ap = R \times K \times LS \tag{1}$$

2.1.1. R-Factor: Rain Erosivity

The influence of climate is directly relevant when predicting erosion values in an area. In this case, precipitation values are crucial due to the erosive capacity. Rainfall generates erosion through direct action mechanisms, where the kinetic energy of raindrops impacts the soil surface, facilitating their disintegration into particles of various sizes that are transported by the simultaneously generated surface runoff. In this study, a total of 10 rain gauge stations with continuous spatiotemporal records of at least twenty years are considered. The average monthly values from each station are collected from the Geographic Information System for Agricultural Data (SIGA) database (https://sig.mapama.gob.es/siga/, accessed on 9 July 2024). To obtain a raster with continuous values, interpolation using the Inverse Distance Weighting (IDW) method is employed [44], using a pixel resolution of 1 × 1 m. This procedure is repeated for all monthly values obtained from the rain gauge stations.

Next, to determine the erosive capacity, the Modified Fournier Index (MFI) is calculated (Equation (2)), where p_i is the amount of precipitation for each month (in mm) and Pt is the annual average precipitation (in mm) [45]. This approach was chosen because, in areas with limited data availability or regions lacking detailed rainfall intensity records, the Modified Fournier Index (MFI) provides an effective approximation for calculating the rainfall erosivity factor (R-Factor). The MFI was proposed as a refinement of the original Fournier Index, as it allows consideration not only of the precipitation during the wettest month but also the precipitation of the remaining months, thereby offering a more comprehensive measure of rainfall aggressiveness and its erosive potential [45]. Finally, the rainfall erosivity index (R-Factor) is calculated using Equation (3). This equation is derived based on the national zoning established by the Institute for Nature Conservation (ICONA) and is based on isoerodent or iso-R mapping [46].

$$\mathrm{MFI} = \Sigma_{i=1}^{12} \frac{p_i^2}{Pt} \tag{2}$$

$$\mathrm{R} = 2.56 \times \mathrm{MFI}^{1.065} \tag{3}$$

2.1.2. K-Factor: Soil Erodibility

Soil erodibility, represented by the K-Factor, refers to the vulnerability or susceptibility of soil to erosion. This factor is influenced by the physical characteristics of the soil, such as texture, structure, permeability, and organic matter content [21]. These parameters are crucial for estimating soil behavior in response to erosion. Additionally, the nature of the parent rock is important, as it accounts for the varying resistance to erosive processes of different geological formations.

The determination of this parameter can be achieved through chemical and granulometric analyses of each soil type studied, followed by applying those results to the Wischmeier nomogram [21]. In this case, the average K values were obtained from data calculated in experimental plots of the erosive lithofacies determined for the province of Pontevedra based on the physical and compositional characteristics of the surface rock layers (Table 1) [47].

Table 1. K-Factor values from the study area were obtained from erosive lithofacies.

Erosive Lithofacies	Values
Consolidated deposits (alluvial fans and marine terraces)	0.166
Unconsolidated deposits (beaches, dunes, marshes, valley bottoms, river terraces and glacis)	0.190
Metamorphic rocks	0.209
Plutonic rocks	0.139

2.1.3. LS-Factor: Topographic Factor

Detailed knowledge of the terrain in the study area is crucial for calculating soil erosion. Areas where surface runoff accumulates with greater volume and velocity exhibit higher erosive potential. These zones are primarily influenced by slope (S-Subfactor) and slope length (L-Subfactor). From a physical standpoint, LS-Factor refers to the horizontal distance over which water moves downslope before significant deposition or a change in flow occurs. As slope length increases, so does the volume of water that accumulates and, therefore, its capacity to erode soil. Flow accumulation, on the other hand, refers to the volume of water that accumulates at a given point on the slope. This volume is a function of both the amount of water that precipitates and the geometry of the watershed and slope. Areas with greater flow accumulation often coincide with areas where slope length is greater, which reinforces the erosive capacity due to an increase in flow velocity and volume [21].

Firstly, the S-Subfactor is computed by generating a slope raster from the Digital Terrain Model (DTM) at a resolution of 1×1 m per pixel and converting slope values to radians using raster calculator tools. For the L-Subfactor, an initial flow accumulation raster is obtained. Given that initial flow accumulation values may be exaggerated, a conversion is performed, limiting the maximum slope length to 250 m, equivalent to 250 cells in our case.

Two rasters, A and B, are generated for processing the flow accumulation raster. In raster A, the flow accumulation raster is reclassified such that values ≥ 250 are set to 0 and values ≤ 250 are set to 1. The raster A is then multiplied by the flow accumulation raster, adjusting pixels with values above 250 to 0 while retaining the original values for pixels ≤ 250. Subsequently, raster B is created where the initial flow accumulation raster is reclassified: values ≤ 250 are set to 250, and values ≥ 250 are set to 0. Finally, raster A and B are added together to produce a final raster where pixels ≤ 250 maintain their original values, and pixels originally exceeding 250, which were exaggerated, are adjusted to 250.

With both subfactors obtained, the LS-Factor value is calculated using Equation (4) [48].

$$LS = \left(Flow\ accumulaion\ \times cell\frac{size}{22.14}\right)^{0.14} \times \left(\frac{sinslope}{0.0896}\right)^{1.3} \quad (4)$$

2.2. Real Erosion Mapping

This mapping assesses the current degree of soil loss in the study area. Therefore, it is necessary to introduce two new factors concerning the current state of the territory in terms of vegetation (C-Factor) and conservation practices (P-Factor). Using the RUSLE equation (citation), these two new factors are added to those already developed in Section 2.1 (Equation (5)).

$$A = R \times K \times LS \times C \times P \quad (5)$$

2.2.1. C-Factor: Soil Cover Factor

The determination of the C-Factor involved generating a physiographic domain map by synthesizing units from the Spanish Forest Map (MFE) of Galicia at a scale of 1:25,000 (Ministry of Ecological Transition and Demographic Challenge (MITECO), https://www.miteco.gob.es/es/cartografia-y-sig/ide/descargas/biodiversidad/mfe.html, accessed on 5 July 2024). Each domain was assigned a C value based on the type of cover (tree or shrub), vegetation density, and the percentage of herbaceous or plant residues (Table 2) [21,49–51]. These values were further refined and validated through direct field observations, ensuring that they accurately reflect the local environmental conditions. The combination of bibliographic data and field observations provided a robust basis for the assignment of C-Factor values in the study area [21,49–51].

Table 2. C-Factor value for the study area for each different cover.

Vegetation Cover Type		C Value
Forest	Pinewood	0.003
	Eucalyptus	0.003
	Oak Grove	0.003
	Eucalyptus, pine, and deciduous forest	0.003
	Pinewood and scattered formations	0.012
	Riparian forest	0.012
	Transitional forest and shrubs	0.014
	Very low-density bush formations	0.26
Crops and grasslands	Vineyards	0.15
	Irrigated crops and pastures	0.14
Wetlands	Wetlands, river channels, and lagoons	0
No vegetation	Urban centers	0.0003
	Discontinuous urbanism	0.002
	Cliffs and rocks	1

2.2.2. P-Factor: Soil Conservation Practices

P-Factor is used in cases where active soil conservation techniques are employed in the study area. The objective of this study is to understand soil potential and actual losses based on purely natural phenomena. Anthropogenic activities can accentuate potential soil losses, whereas in cases where protective measures or activities are developed, these erosion rates can be mitigated. Since the P-Factor reduces the erosion results obtained through RUSLE (Equation (5)), it is assigned a value of 1.

3. Results

3.1. Potential Erosion

3.1.1. R-Factor Values

The values obtained from the calculation of the R-Factor show a range of results from 1216 mm to a maximum of 1627 mm (Figure 3). The variability in the data indicates that areas with greater precipitation influence are in the N–NW zone, notably affecting Isla de Arosa, the municipal area of Villanueva de Arosa, and the NW sector of the El Grove Peninsula. Moving southeast from these areas, there is a significant decrease in R values, with the lowest values observed in the metropolitan area of Sanjenjo. These results were derived from the interpolation of rainfall data from 10 stations with continuous records of at least 20 years using the Inverse Distance Weighting (IDW) method. The relationship between these rainfall values and rainfall erosivity is crucial for understanding the spatial distribution of potential erosion in the study area, where the R-Factor plays a particularly significant role.

3.1.2. K-Factor Values

The study area is divided into four distinct erosive lithofacies defined based on the physical and compositional characteristics of the surface rock layers (Figure 4A) [47]. These include soils over granitic rocks, metamorphic rocks, consolidated Quaternary deposits, and unconsolidated Quaternary deposits. The highest average values of K are found in soils over plutonic rocks (0.139), while values are highest over metamorphic lithologies (0.209) and unconsolidated deposits (0.190) (Figure 4B). The relationship between these K values and the physical and geological characteristics of the soils is essential for understanding soil erodibility and its contribution to potential erosion in the study area.

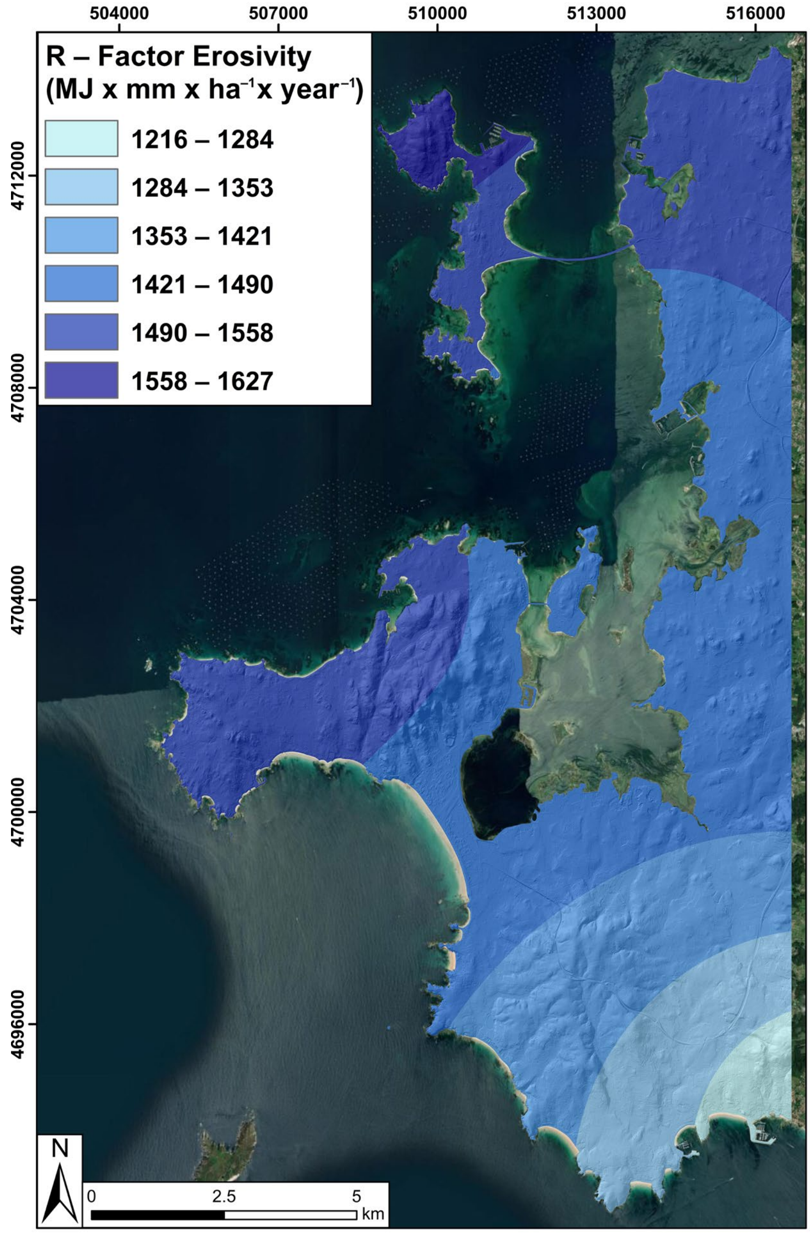

Figure 3. R-Factor values for the SE of the Ría de Arosa.

3.1.3. LS-Factor Values

The result of the relationship between the L and S Subfactors is shown in Figure 5. These results were obtained by generating raster layers of slope and flow accumulation from the 1 × 1 m Digital Elevation Model (DEM). The terrain topography exhibits two distinct zones. The highest LS values are concentrated in areas dominated by granitic and metamorphic lithostructural reliefs. The interior of the El Grove Peninsula, characterized by granitic dome structures, crests, and peaks, features steep slopes, which contribute to higher LS values. The internal zones of the Castrove Peninsula, coinciding with metamorphic lithostructural reliefs, show intermediate values, increasing as the slopes become steeper along small river valley incisions [39,40]. The rest of the area generally presents low values where they coincide with alluvial fan systems, marine and river terraces, as well as coastal deposits (beaches, bars, marshes, and dune systems). Finally, cliffs located in the S-SW area, where metamorphic rock outcrops are predominant, show intermediate to high values due to their significant slopes. The relationship between these LS values and the terrain's topographic characteristics is crucial for understanding the spatial distribution of potential and actual erosion in the study area.

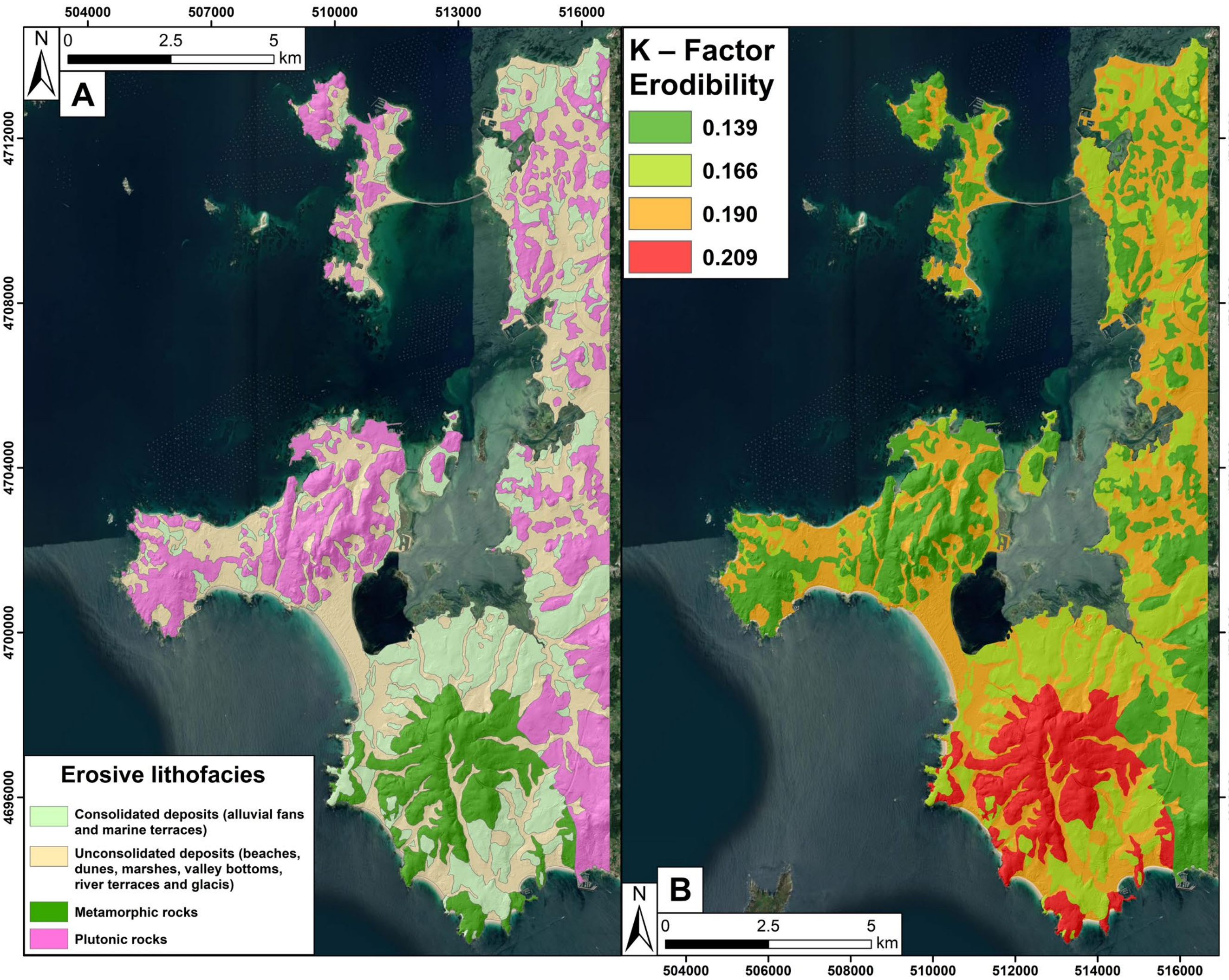

Figure 4. (**A**) Erosive lithofacies. (**B**) K-Factor values for the SE of the Ría de Arosa.

3.1.4. Potential Erosion Risk of SE Ría de Arosa

The potential erosion map is generated by multiplying the factors R, K, and LS (Wischmeier et al., 1978 [21]), as previously described (Figure 6). Once obtained, these values are reclassified according to intervals established by the Food and Agriculture Organization of the United Nations (FAO) [11], which have been detailed in subsequent articles [30,31]. The values are classified into seven stages of erosion levels, ranging from very low to extreme, expressed in metric tons per hectare per year (t/ha/year) (Tables 3 and 4). To calculate approximate soil losses in millimeters per year, the mean values of soil bulk density (1.3 g/cm^3) [52–54] (Table 3) and the approximate mean soil bulk density calculated for the study area (1.0 g/cm^3) [55] (Table 4) were used.

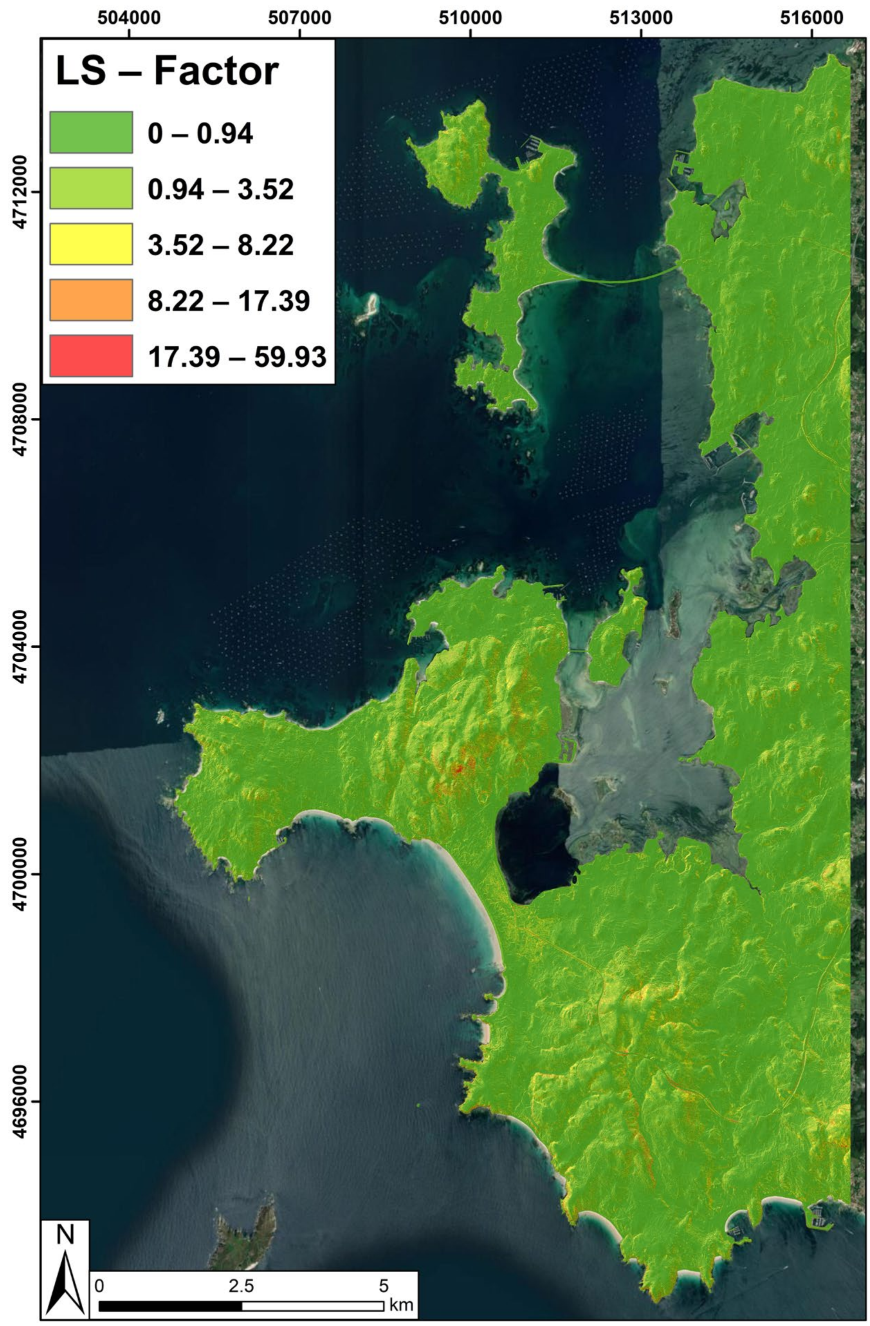

Figure 5. LS-Factor values for the SE of the Ría de Arosa.

Table 3. Soil loss values (mm/year) based on a soil bulk density of 1.3 g/cm^3 [52–54].

Class	t/ha/year	mm/year
Very low erosion and tolerable soil loss	<5	<0.38
Low erosion and tolerable soil loss	5–10	0.38–0.77
Mild erosion level	10–25	0.77–1.92
Moderate erosion level	25–50	1.92–3.85
Severe erosion level	50–100	3.85–7.69
Very severe erosion level	100–200	7.69–15.38
Extreme erosion level	>200	>15.38

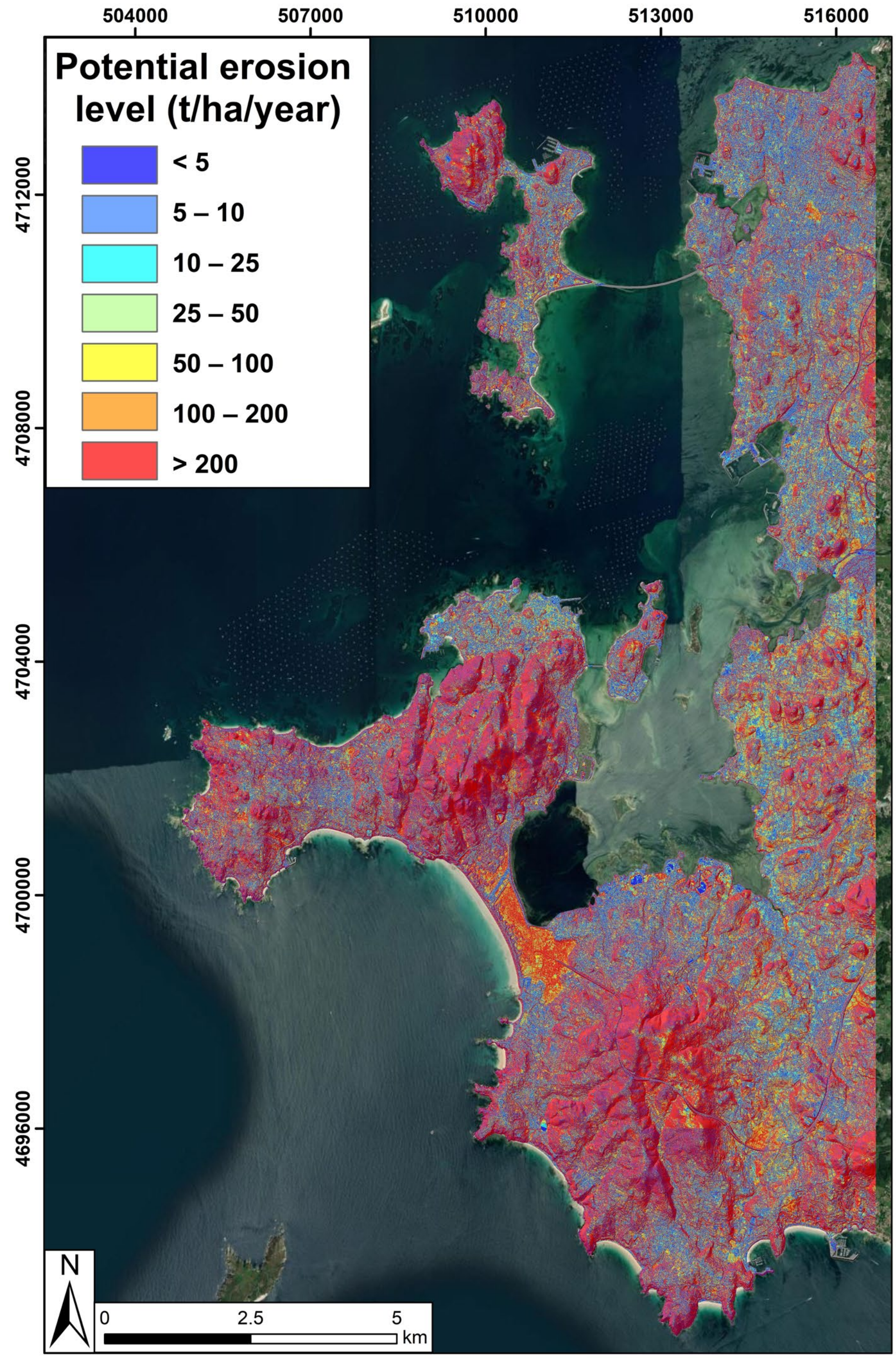

Figure 6. Potential erosion map of SE Ría de Arosa.

Table 4. Soil loss values (mm/year) based on a soil bulk density of 1.0 g/cm^3 [55].

Class	t/ha/year	mm/year
Very low erosion and tolerable soil loss	<5	<0.50
Low erosion and tolerable soil loss	5–10	0.50–1.00
Mild erosion level	10–25	1.00–2.50
Moderate erosion level	25–50	2.50–5.00
Severe erosion level	50–100	5.00–10.00
Very severe erosion level	100–200	10.00–20.00
Extreme erosion level	>200	>20.00

On the southeastern margin of the Ría de Arosa, diverse erosion results are observed. To aid understanding, distinctions are made between inland and coastal zones. In the inland areas, elevated erosion values are notable in residual reliefs of igneous and metamorphic rocks, characterized by steep slopes. These areas are primarily located within the El Grove Peninsula (granitic domes, ridges, crests, and peaks) and Castrove Peninsula (metamorphic rocks), exhibiting erosion levels ranging from severe to extreme (Figure 6) (Tables 3 and 4).

Transitional environments toward the coast, where slopes gradually decrease and morphologies are gentler, show lower erosion values. These zones are characterized by landforms such as alluvial fans, cones, or marine terraces indicating former coastal positions, displaying erosion values ranging from moderate to very low (Figure 6) (Tables 3 and 4).

The coastal environment features depositional settings (beaches, dunes, marshes, and tombolos) and erosive environments (cliffs). In the latter, due to steep slopes, the highest erosion values are concentrated, varying from very high to extreme levels.

3.2. Real Erosion

3.2.1. C-Factor Values

The classification of the study area into physiognomic domains (Figure 7A) allows for assigning specific values of the C-Factor to each of them (Figure 7B). The characteristics of the area indicate that a greater percentage of the land is covered by vegetation. Within these domains, a distinction is made between forests, crops, grasslands, wetlands, and areas without vegetation.

In the forests category, there are notable differences between various types, with pine forests, eucalyptus forests, and mixed forests (eucalyptus and deciduous species) being prominent. These lush forests, located in areas dominated by granitic and metamorphic rocks, receive a C-Factor value of 0.003. They thrive on more acidic soils developed over granitic and metamorphic lithologies, which are well represented in the interior of the El Grove and Castrove Peninsulas or on the Isle of Arosa.

The riparian forest zones, where vegetation density is lower, and transition zones with scattered bushes receive C-Factor values of 0.012. These areas are located on the edges of coastal zones and serve as a transition to the much denser interior forests. The environment around the Lanzada tombolo, characterized by sparse and scattered shrub formations, receives the highest value of the C-Factor for vegetated surfaces: 0.26.

The area is predominantly covered by agricultural land, primarily cultivated with vineyards. Vineyards, which sometimes include intercalations of trees or other crops, are assigned a C-Factor value of 0.15. Pasture areas, often poorly consolidated and of low density, have a C-Factor value of 0.14.

There are two distinct types within the areas without vegetation. Firstly, urbanized zones have very low C-Factor values. In well-defined urban cores within metropolitan areas, the values are 0.0003. Discontinuous urban areas have C-Factor values of 0.002. On the other hand, in coastal zones where no vegetation is present (such as beaches or cliffs), the C-Factor value is 1.

3.2.2. Real Erosion Risk of SE Ría de Arosa

The mapping of actual erosion is generated using the RUSLE equation, which integrates erosivity (R-Factor), erodibility (K-Factor), slope length and steepness (LS-Factor), and land use or land cover (C-Factor) [21]. Like the potential erosion mapping, it undergoes a reclassification into seven classes using the same erosion value equivalencies (Tables 3 and 4).

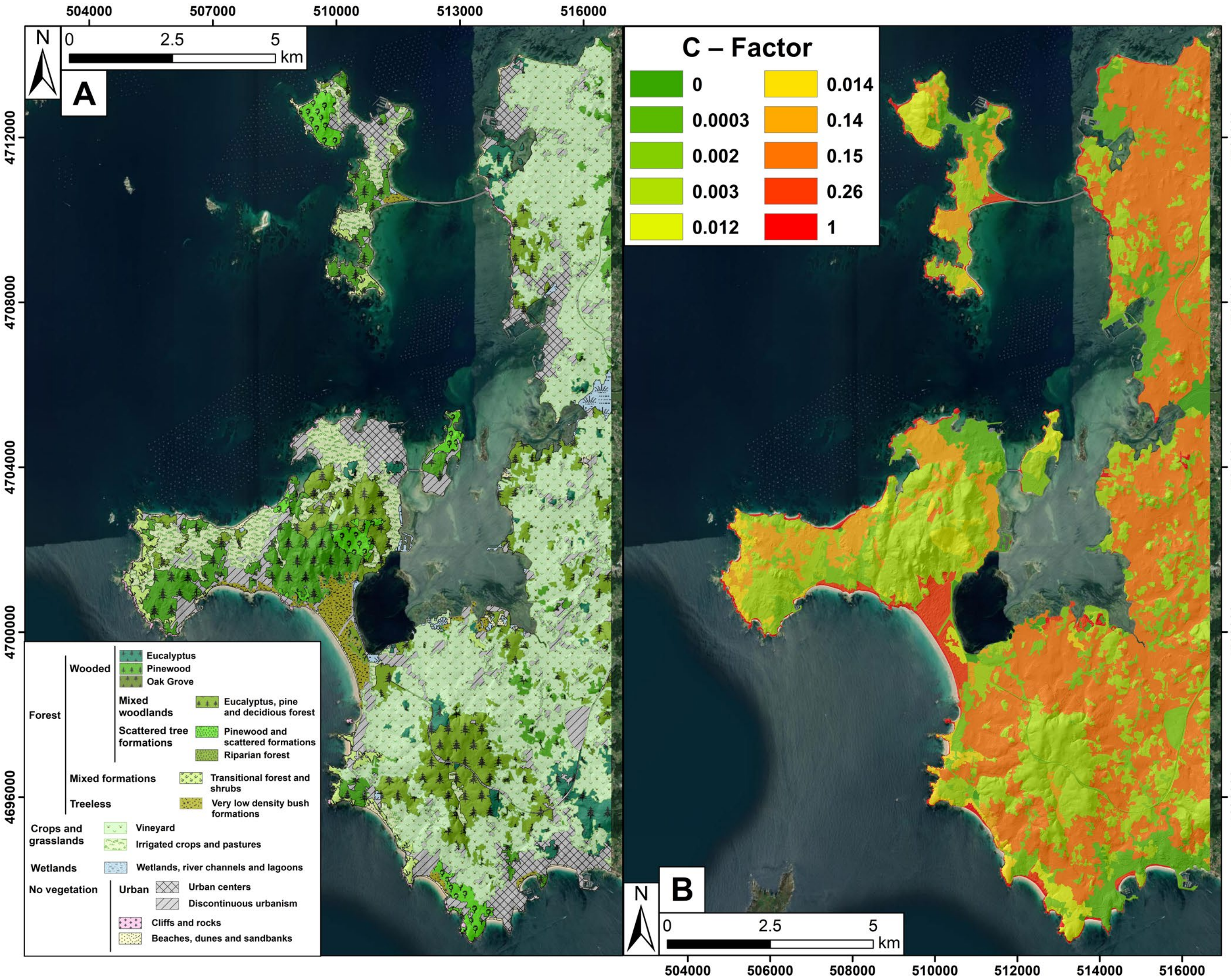

Figure 7. (**A**) Physiognomy domains obtained from the Spanish forest map. (**B**) C-Factor values for the SE of the Ría de Arosa.

The distribution of results shows a predominance of low to very low erosion levels (Figure 8). In inland areas where steep slopes are prevalent, the presence of dense forests (pine or eucalyptus) significantly reduces erosion values. On the other hand, less-vegetated areas with steeper slopes exhibit higher erosion values. The most critical zones, with very high erosion levels, are in the central part of the El Grove Peninsula, characterized by a low density of shrub species and a substrate covered with plant debris and fresh rock, where erosion values range from very high to extreme.

Associated with the coastal environment, very high and extreme erosion values are recorded in cliff areas. Near the Tómbolo de la Lanzada, erosion values are generally moderate; however, on the slopes of the dunes, where there are steep changes in slope, significant erosion values are reached.

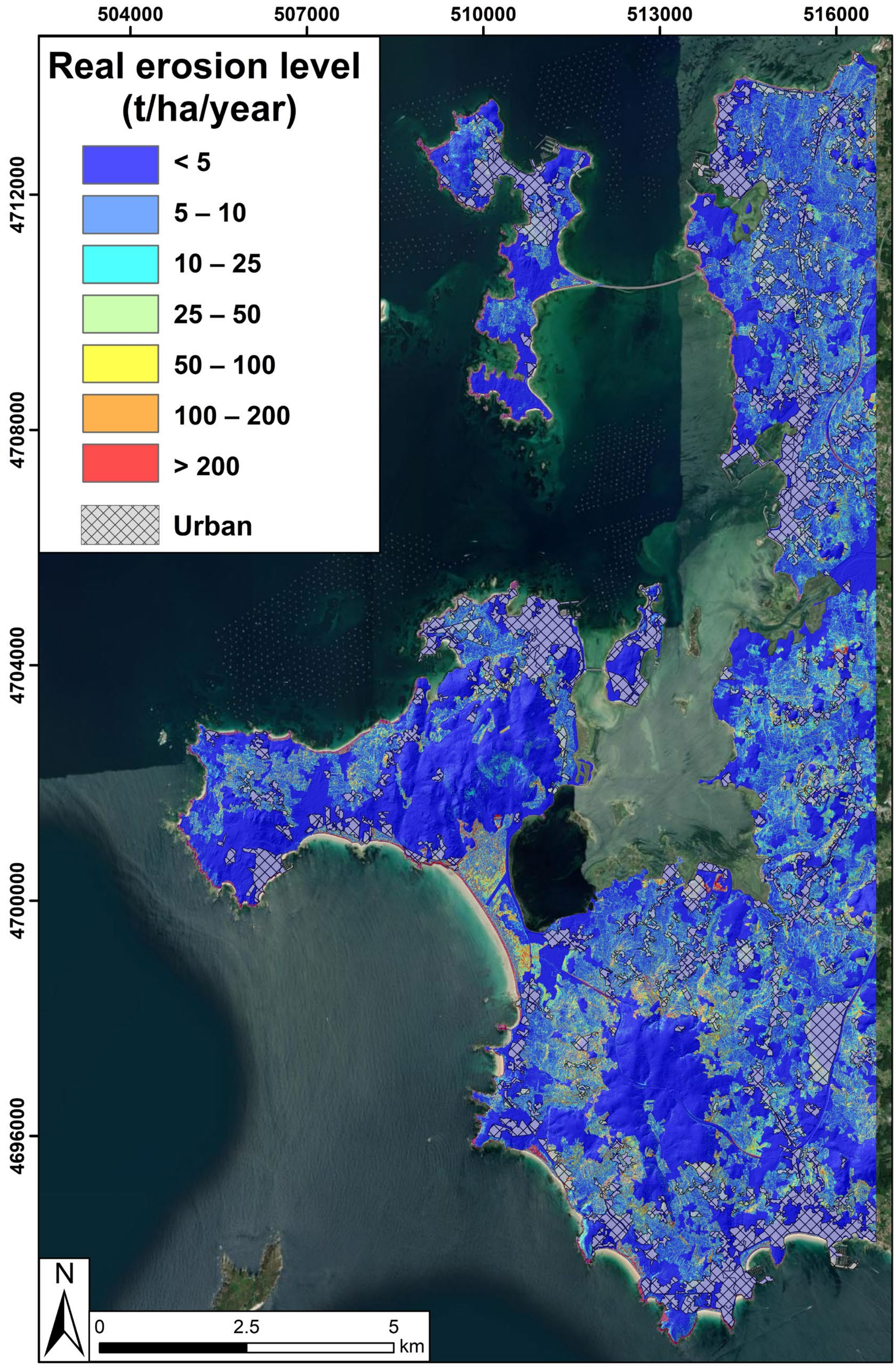

Figure 8. Real erosion map of SE Ría de Arosa.

4. Discussion

4.1. Comparison of Potential and Actual Erosion Cartographies

The comparison between potential and actual erosion maps highlights the significant influence of vegetation cover on soil and water erosion values. Potential erosion (Figure 6), which considers erosivity (R-Factor), erodibility (K-Factor), and topography (LS-Factor), demonstrates how higher soil loss values concentrate in areas with steeper slopes and highly erodible soils. The R-Factor, although relatively high compared to other values in the Iberian Peninsula, does not show a clear trend indicating a uniform increase or decrease in erosion across the study area. However, it is important to clarify that higher R-Factor values facilitate increased soil loss in erosion-prone areas.

It is observed that very high values are mainly concentrated in cliff zones, residual granite, and metamorphic reliefs, as well as areas with soils developed on less compact lithologies (such as beaches, tombolos, or marshes). These high values range from severe (>50 t/ha/year) to extreme (>200 t/ha/year).

The map of actual erosion (Figure 8), incorporating the land cover and land use factor (C-Factor), indicates a significant moderating effect on erosion levels. Areas dominated by forest cover (pine, eucalyptus, or oak forests) show a notable decrease in soil loss values. Here, a clear transition from severe to low or very low erosion (<10 t/ha/year) can be observed. This underscores the importance of such vegetation covers in mitigating the erosive impact of rainfall.

Transition zones from forest to grassland, characterized by scattered shrubs or areas cultivated with vineyards, exhibit an increase in erosion values. In these areas, where topographic factors are more pronounced or soils are less compact, higher values of actual erosion are detected. Therefore, vegetation cover emerges as a crucial element in reducing erosion, whereas a lack of vegetation and adverse topographic conditions enhance erosive risk.

4.2. Analysis of Erosion Risks in Relation to Land Uses

To analyze the areas most exposed to soil loss based on land uses, values of erosion exceeding 50 t/ha/year are overlaid into the Spanish Land Use Information System (SIOSE) layer (Figure 9A). This facilitates the identification of locations with higher erosion risk. Generally, it is observed that areas with the highest concentration of elevated values are found in coastal zones lacking vegetation.

Different locations have been selected to provide a more detailed description of this phenomenon. On the N-NE flank of the El Grove peninsula (Figure 9B), very high erosion values are recorded in peripheral areas near human-impacted zones such as ports or Wastewater Treatment Plants (WWTP). The coastal area between Cape Fagilda and Montalvo (Figure 9C) also shows high erosion values in locations near residential areas.

In more inland areas away from the coastal environment, high erosion values are observed in vineyard fields where slopes are slightly steeper. Finally, the area where erosion risk is most pronounced is in the coastal surroundings south of the municipality of Portonovo (Figure 9D), with elevated erosion values on cliffs where parts of the urban center are located.

4.3. Evaluation of Erosion in Protected Natural Areas

In the study area, in relation to the intertidal environment along this coastline, the protected natural spaces of the Ons–O Grove and Umia–O Grove complexes (Special Bird Protection Area, ZEPA) are situated. To identify the areas most affected by soil loss due to water erosion, values exceeding 50 t/ha/year are overlaid onto the protected zones (Figure 10A). The area most affected by erosion is found at the La Lanzada Tombolo (Figure 10B). This area features sparse and scattered shrubby and herbaceous vegetation on loosely compacted or non-compacted substrates (dunes, beaches, and tidal bars). Protecting this environment is crucial due to its natural characteristics and its role as a land connection to the El Grove Peninsula.

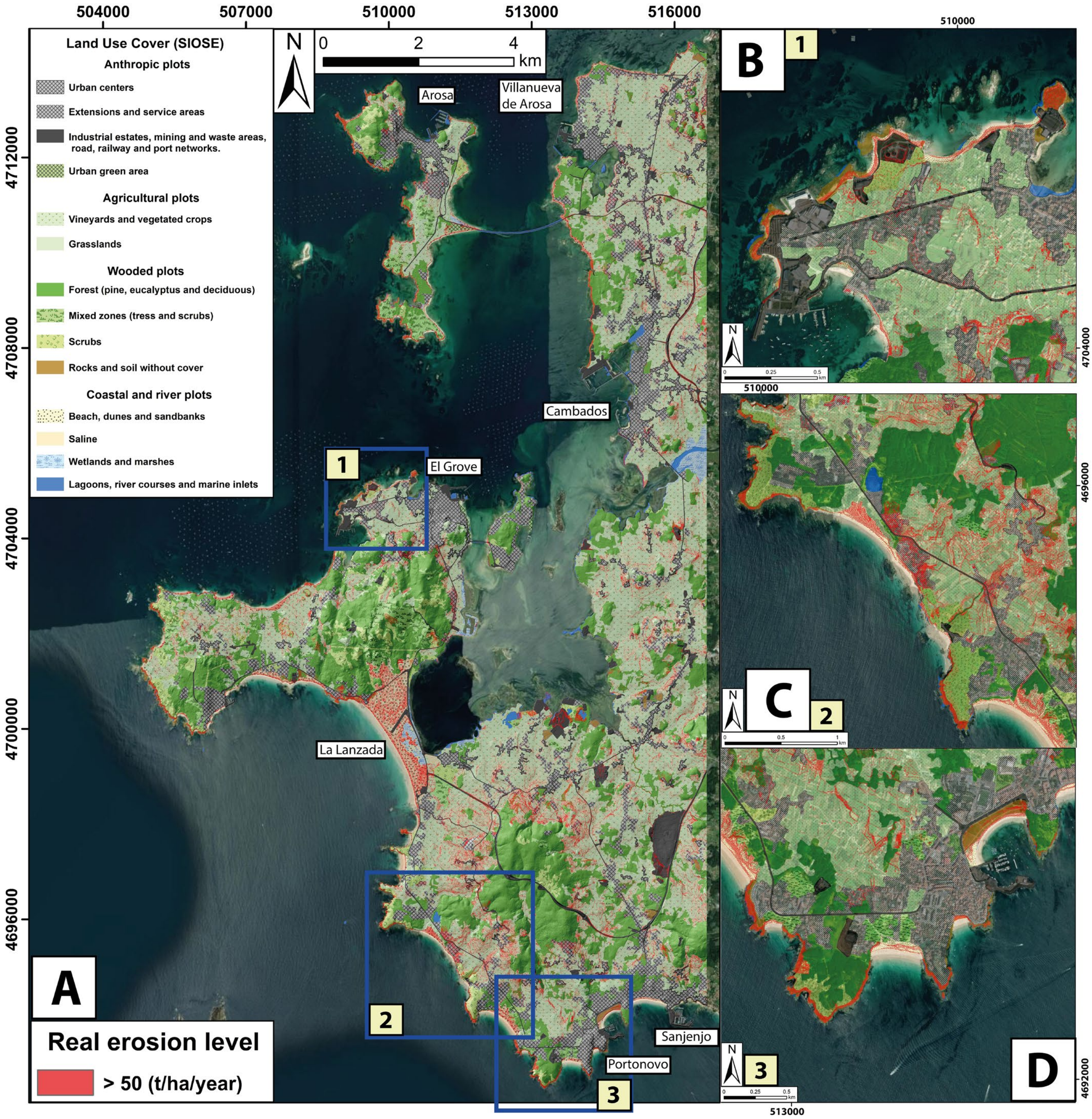

Figure 9. (**A**) Real erosion values > 50 t/ha/year on the SIOSE layer. (**B**) N-NE flank of the El Grove Peninsula. (**C**) Coastal area between Capes Fagilda and Montalvo. (**D**) Coastal environment south of Portonovo.

The western coastal flank of the El Grove Peninsula records very high erosion values due to coastal features (Figure 10C). These areas have lower population density and less vegetated surfaces, often with very steep slopes. In the south of Arosa Island, although less populated, there are defined protected natural areas (Figure 10D). The entire coastal environment exhibits significant erosion values that could adversely impact the proper preservation of wetlands.

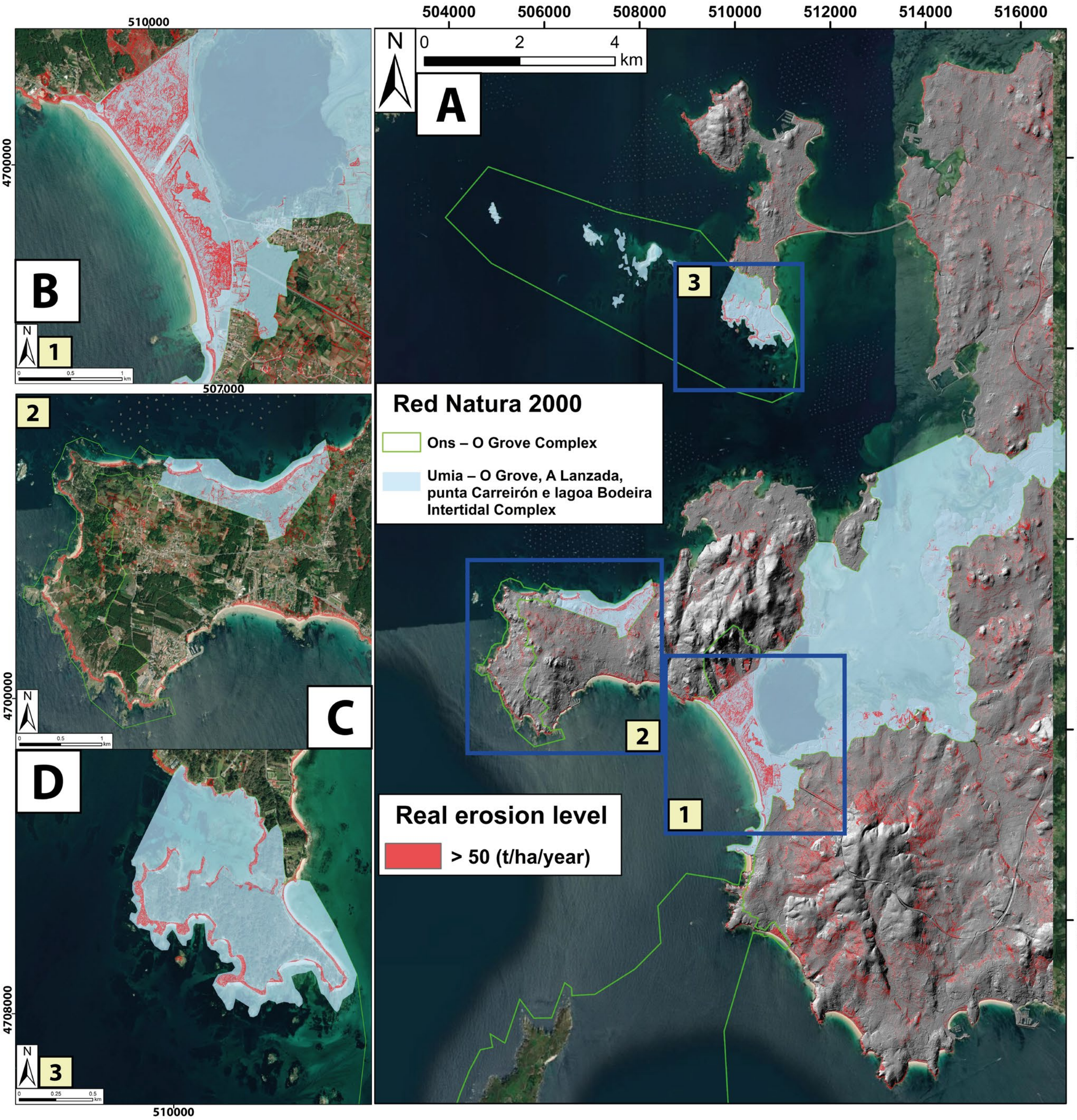

Figure 10. (**A**) Real erosion values > 50 t/ha/year on the layer of protected natural spaces. (**B**) Tómbolo de La Lanzada. (**C**) Coastal flank west of the El Grove Peninsula. (**D**) South of the Island of Arosa.

4.4. Corrective Measures and Mitigation Strategies for Soil Erosion in the SE of the Ría de Arosa

Once the areas most affected by soil loss due to water erosion have been identified, proposals for potential corrective or mitigating measures can be developed. From a technical standpoint, the factors that can be addressed more easily and effectively are topography, land cover, and use. In the study area, it has been observed that higher erosion values occur in areas where bare soils or low-density vegetation coincide with steep slopes.

The La Lanzada Tombolo (Figure 10B), where sandy substrate from coastal action is concentrated, exhibits elevated erosion values, highlighting the need for various protective conservation and restoration measures. The implementation of metal mesh fences is an economical and sustainable measure for coastal restoration and protection. These fences reduce wind and runoff energy, promoting sediment accumulation and slope stabilization [56–58]. Moreover, they represent a long-term strategy considering the increasing frequency of extreme weather events [5,6]. Additionally, dune fields can be replanted with native shrub species and grasses that retain sediment and water. This action also improves soil properties by increasing the content of organic matter and improving plant biodiversity [59]. All areas adjacent to La Lanzada, particularly those that host protected wetlands, must be periodically monitored due to their status as priority areas for conservation [60]. When necessary, protective measures aligned with these strategies should be implemented to guarantee the preservation of these places of special biodiversity.

In cliffy areas, water erosion results from both rainfall and coastal processes. Therefore, it would be beneficial to conduct supplementary studies specifically focusing on coastal erosion in those areas where water erosion values are high [61]. In some cases, it may be necessary to consider beach widening measures to mitigate direct wave impact, thereby increasing sedimentation rates or reducing wave energy [62]. Subsequently, stabilizing the slope and potentially revegetating it could be considered.

Another problematic area is found in the agricultural zone of vineyard cultivation, where slopes are slightly elevated (Figure 9B). One effective measure, where topography allows, is the construction of agricultural terraces. These terraces create a natural break in the slope, forming a stepped morphology that enhances water infiltration and reduces the erosive action of surface runoff. This approach promotes soil stability and improves soil quality [63,64]. In Mediterranean regions where vineyard erosion is a concern, using straw mulch on the soil is being implemented. This practice, which is cost-effective and sustainable, effectively reduces soil erodibility and the impact of runoff [65]. It is particularly suitable for areas with gentle slopes where terrace construction is impractical, or as an alternative due to its quick and straightforward implementation.

5. Conclusions

The present study has identified the most vulnerable areas to water erosion in the southeast of the Ría de Arosa. It provides a detailed analysis of the factors influencing soil loss and proposes corrective measures to mitigate these impacts in key locations. Here are the main findings and recommendations summarized:

1. Areas with severe to extreme erosion values, with soil loss exceeding 50 t/ha/year and reaching more than 200 t/ha/year, are primarily located in coastal zones with steep slopes, poorly developed soils, and sparse vegetation. High erosion values are especially prevalent in cliff areas, steep slopes, and regions with poorly consolidated soils, such as dunes and beaches. Recommended measures for these areas include the installation of metal mesh fences and reforestation with native plant species to stabilize the soil and reduce sediment loss. Additionally, it is suggested to conduct further studies on wind and coastal erosion (dune systems and cliffs) in these problematic areas.
2. Erosion values in areas ranging between 10.1 and 50 t/ha/year include cultivated lands such as vineyards and transition zones between forests and grasslands. Additionally, some vineyards in the study area also exhibit severe to extreme erosion values due to steep terrain and insufficient soil protection. Recommended measures include the construction of agricultural terraces and the use of straw mulch to improve soil stability and mitigate erosion.
3. Areas with erosion values up to 10 t/ha/year have better-developed soils and denser vegetation, providing good protection against erosion. Despite the lower erosion levels, maintaining conservation practices is crucial to preserving soil stability. Reforestation with native species is particularly important during post-fire periods when soil erosion rates are elevated.

The potential and actual erosion maps have facilitated the precise identification of the most affected areas, allowing for the implementation of specific conservation measures. Reducing slope length and steepness through contour cultivation and terracing is presented as an effective and low-cost strategy for soil protection. Applying these specific strategies for each type of area will help reduce soil loss, protect ecosystems, and promote sustainability in this vulnerable coastal region. Effective implementation of these recommendations is crucial for ensuring the long-term conservation of this coastal environment.

Author Contributions: Conceptualization, C.E.N., A.M.M.-G. and L.M.; methodology, C.E.N. and A.M.M.-G.; software, C.E.N.; validation, C.E.N. and A.M.M.-G.; formal analysis, C.E.N., A.M.M.-G. and L.M.; investigation, C.E.N. and A.M.M.-G.; resources, C.E.N., A.M.M.-G. and L.M.; data curation, C.E.N., A.M.M.-G. and L.M.; writing—original draft preparation, C.E.N. and A.M.M.-G.; writing—review and editing, A.M.M.-G.; visualization, C.E.N. and A.M.M.-G.; supervision, A.M.M.-G.; project administration, A.M.M.-G.; funding acquisition, A.M.M.-G. All authors have read and agreed to the published version of the manuscript.

Funding: Grant 131874B–I00 is funded by MCIN/AEI/10.13039/501100011033—Ministry for the Ecological Transition and the Demographic Challenge.

Informed Consent Statement: Not applicable.

Data Availability Statement: The data presented in this study are available within this article.

Acknowledgments: This research was assisted by the GEAPAGE research group (Environmental Geomorphology and Geological Heritage) of the University of Salamanca.

Conflicts of Interest: The authors declare no conflicts of interest.

References

1. Martínez, M.L.; Intralawan, A.; Vázquez, G.; Pérez-Maqueo, O.; Sutton, P.; Landgrave, R. The Coasts of Our World: Ecological, Economic and Social Importance. *Ecol. Econ.* **2007**, *63*, 254–272. [CrossRef]
2. Burke, L.; Kura, Y. *Pilot Analysis of Global Ecosystems: Coastal Ecosystems*; World Resources Institute: Washington, DC, USA, 2000.
3. Li, K.; Zhang, L.; Chen, B.; Zuo, J.; Yang, F.; Li, L. Analysis of China's Coastline Changes during 1990–2020. *Remote Sens.* **2023**, *15*, 981. [CrossRef]
4. Jin, X.; Luan, W.; Yang, J.; Yue, W.; Wan, S.; Yang, D.; Xiao, X.; Xue, B.; Dou, Y.; Lyu, F.; et al. From the Coast to the Interior: Global Economic Evolution Patterns and Mechanisms. *Humanit. Soc. Sci. Commun.* **2023**, *10*, 723. [CrossRef]
5. Lee, H.; Calvin, K.; Dasgupta, D.; Krinner, G.; Mukherji, A.; Thorne, P.; Trisos, C.; Romero, J.; Aldunce, P.; Barret, K. IPCC 2023: Climate Change 2023: Synthesis Report, Summary for Policymakers. In *Contribution of Working Groups I, II and III to the Sixth Assessment Report of the Intergovernmental Panel on Climate Change*; Core Writing Team, Lee, H., Romero, J., Eds.; IPCC: Geneva, Switzerland, 2023.
6. Nicholls, R.J.; Lincke, D.; Hinkel, J.; Brown, S.; Vafeidis, A.T.; Meyssignac, B.; Hanson, S.E.; Merkens, J.-L.; Fang, J. A Global Analysis of Subsidence, Relative Sea-Level Change and Coastal Flood Exposure. *Nat. Clim. Chang.* **2021**, *11*, 338–342. [CrossRef]
7. Eekhout, J.P.C.; De Vente, J. Global Impact of Climate Change on Soil Erosion and Potential for Adaptation through Soil Conservation. *Earth-Sci. Rev.* **2022**, *226*, 103921. [CrossRef]
8. Pal, S.C.; Chakrabortty, R.; Towfiqul Islam, A.R.M.; Roy, P.; Chowdhuri, I.; Saha, A.; Islam, A.; Costache, R.; Alam, E. Land Use and Climate Change-Induced Soil Erosion Mapping in a Sub-Tropical Environment. *Geomat. Nat. Hazards Risk* **2023**, *14*, 2270129. [CrossRef]
9. Mohammed, S.; Abdo, H.G.; Szabo, S.; Pham, Q.B.; Holb, I.J.; Linh, N.T.T.; Anh, D.T.; Alsafadi, K.; Mokhtar, A.; Kbibo, I.; et al. Estimating Human Impacts on Soil Erosion Considering Different Hillslope Inclinations and Land Uses in the Coastal Region of Syria. *Water* **2020**, *12*, 2786. [CrossRef]
10. O'Riordan, R.; Davies, J.; Stevens, C.; Quinton, J.N.; Boyko, C. The Ecosystem Services of Urban Soils: A Review. *Geoderma* **2021**, *395*, 115076. [CrossRef]
11. Food and Agriculture Organization of the United Nations. *Status of the World's Soil Resources: Technical Summary*; Food and Agriculture Organization of the United Nations: Rome, Italy, 2015.
12. Montanarella, L.; Pennock, D.J.; McKenzie, N.; Badraoui, M.; Chude, V.; Baptista, I.; Mamo, T.; Yemefack, M.; Singh Aulakh, M.; Yagi, K.; et al. World's Soils Are under Threat. *Soil* **2016**, *2*, 79–82. [CrossRef]
13. Borrelli, P.; Robinson, D.A.; Fleischer, L.R.; Lugato, E.; Ballabio, C.; Alewell, C.; Meusburger, K.; Modugno, S.; Schütt, B.; Ferro, V.; et al. An Assessment of the Global Impact of 21st Century Land Use Change on Soil Erosion. *Nat. Commun.* **2017**, *8*, 2013. [CrossRef]
14. Borrelli, P.; Robinson, D.A.; Panagos, P.; Lugato, E.; Yang, J.E.; Alewell, C.; Wuepper, D.; Montanarella, L.; Ballabio, C. Land Use and Climate Change Impacts on Global Soil Erosion by Water (2015–2070). *Proc. Natl. Acad. Sci. USA* **2020**, *117*, 21994–22001. [CrossRef]
15. Lal, R. Soil Carbon Sequestration Impacts on Global Climate Change and Food Security. *Science* **2004**, *304*, 1623–1627. [CrossRef]

16. O'Neal, M.R.; Nearing, M.A.; Vining, R.C.; Southworth, J.; Pfeifer, R.A. Climate Change Impacts on Soil Erosion in Midwest United States with Changes in Crop Management. *CATENA* **2005**, *61*, 165–184. [CrossRef]
17. Montgomery, D.R. Soil Erosion and Agricultural Sustainability. *Proc. Natl. Acad. Sci. USA* **2007**, *104*, 13268–13272. [CrossRef]
18. Cook, H.L. The Nature and Controlling Variables of the Water Erosion Process. *Soil Sci. Soc. Am. J.* **1937**, *1*, 487–494. [CrossRef]
19. Kirkby, M.J.; Morgan, R.P.C. *Soil Erosion*; Wiley: New York, NY, USA, 1981; p. 312.
20. Morgan, R.P.C.; Nearing, M. *Handbook of Erosion Modelling*; John Wiley & Sons: Hoboken, NJ, USA, 2016.
21. Wischmeier, W.H.; Smith, D.D. *Predicting Rainfall Erosión Losses: A Guide to Conservation Planning (No. 537)*; Department of Agriculture, Science and Education Administration: Washinton, DC, USA, 1978.
22. Laflen, J.M.; Lane, L.J.; Foster, G.R. WEPP: A New Generation of Erosion Prediction Technology. *J. Soil Water Conserv.* **1991**, *46*, 34.
23. Santhi, C.; Arnold, J.G.; Williams, J.R.; Dugas, W.A.; Srinivasan, R.; Hauck, L.M. Validation of the Swat Model on a Large Rwer Basin with Point and Nonpoint Sources. *J. Am. Water Resour. Assoc.* **2001**, *37*, 1169–1188. [CrossRef]
24. Lufafa, A.; Tenywa, M.M.; Isabirye, M.; Majaliwa, M.J.G.; Woomer, P.L. Prediction of Soil Erosion in a Lake Victoria Basin Catchment Using a GIS-Based Universal Soil Loss Model. *Agric. Syst.* **2003**, *76*, 883–894. [CrossRef]
25. Parveen, R.; Kumar, U. Integrated Approach of Universal Soil Loss Equation (USLE) and Geographical Information System (GIS) for Soil Loss Risk Assessment in Upper South Koel Basin, Jharkhand. *J. Geogr. Inf. Syst.* **2012**, *4*, 588–596. [CrossRef]
26. Haokip, P.; Khan, M.A.; Choudhari, P.; Kulimushi, L.C.; Qaraev, I. Identification of Erosion-Prone Areas Using Morphometric Parameters, Land Use Land Cover and Multi-Criteria Decision-Making Method: Geo-Informatics Approach. *Environ. Dev. Sustain.* **2022**, *24*, 527–557. [CrossRef]
27. Renard, K.G.; Foster, G.R.; Weesies, G.A. *Predicting Soil Erosion by Water: A Guide to Conservation Planning with the Revised Universal Soil Loss Equation (RUSLE)*; USDA Agricultural Handbook: Washington, DC, USA, 1997; p. 404.
28. Benavidez, R.; Jackson, B.; Maxwell, D.; Norton, K. A Review of the (Revised) Universal Soil Loss Equation ((R)USLE): With a View to Increasing Its Global Applicability and Improving Soil Loss Estimates. *Hydrol. Earth Syst. Sci.* **2018**, *22*, 6059–6086. [CrossRef]
29. Terranova, O.; Antronico, L.; Coscarelli, R.; Iaquinta, P. Soil Erosion Risk Scenarios in the Mediterranean Environment Using RUSLE and GIS: An Application Model for Calabria (Southern Italy). *Geomorphology* **2009**, *112*, 228–245. [CrossRef]
30. Martínez-Graña, A.; Carrillo, J.; Lombana, L.; Criado, M.; Palacios, C. Mapping the Risk of Water Soil Erosion in Larrodrigo (Salamanca, Spain) Using the RUSLE Model and A-DInSAR Technique. *Agronomy* **2021**, *11*, 2120. [CrossRef]
31. Merchán, L.; Martínez-Graña, A.M.; Alonso Rojo, P.; Criado, M. Water Erosion Risk Analysis in the Arribes Del Duero Natural Park (Spain) Using RUSLE and GIS Techniques. *Sustainability* **2023**, *15*, 1627. [CrossRef]
32. Sifi, S.; Aydi, A.; Bouamrane, A.; Zaghdoudi, S.; Gasmi, M. Appraisal of Soil Erosion Risk in Northeastern Tunisia Using Geospatial Data and Integrated Approach of RUSLE Model and GIS. *J. Earth Syst. Sci.* **2024**, *133*, 67. [CrossRef]
33. Fernández, C.; Vega, J.; Jiménez, E.; Vieira, D.; Merino, A.; Ferreiro, A.; Fonturbel, T. Seeding and Mulching+ Seeding Effects on Post-fire Runoff, Soil Erosion and Species Diversity in Galicia (NW Spain). *Land Degrad. Dev.* **2012**, *23*, 150–156. [CrossRef]
34. Vieira, D.C.S.; Borrelli, P.; Jahanianfard, D.; Benali, A.; Scarpa, S.; Panagos, P. Wildfires in Europe: Burned Soils Require Attention. *Environ. Res.* **2023**, *217*, 114936. [CrossRef]
35. Shakesby, R.A. Post-Wildfire Soil Erosion in the Mediterranean: Review and Future Research Directions. *Earth-Sci. Rev.* **2011**, *105*, 71–100. [CrossRef]
36. Moody, J.A.; Shakesby, R.A.; Robichaud, P.R.; Cannon, S.H.; Martin, D.A. Current Research Issues Related to Post-Wildfire Runoff and Erosion Processes. *Earth-Sci. Rev.* **2013**, *122*, 10–37. [CrossRef]
37. Chazarra Bernabé, A.; Lorenzo Mariño, B.; Romero Fresneda, R.; Moreno García, J.V. *Evolución de Los Climas de Köppen en España En El Periodo 1951–2020*; Agencia Estatal de Meteorología: Madrid, Spain, 2022. [CrossRef]
38. Llana-Fúnez, S.; Marcos, A. The Malpica–Lamego Line: A Major Crustal-Scale Shear Zone in the Variscan Belt of Iberia. *J. Struct. Geol.* **2001**, *23*, 1015–1030. [CrossRef]
39. Martínez-Graña, A.M.; Arias, L.; Goy, J.L.; Zazo, C.; Silva, P. Geomorphology of the mouth of the Arosa estuary (Coruña-Pontevedra, Spain). *J. Maps* **2017**, *13*, 554–562. [CrossRef]
40. Nieto, C.E.; Martínez-Graña, A.M.; Merchán, L. Landscape Analysis and Coastal Planning: Ría de Arosa (Pontevedra, Spain). *Land* **2024**, *13*, 645. [CrossRef]
41. Macías, F.; Calvo de Anta, R. Los Suelos. In *Atlas de Galicia*; Sociedade para o Desenvolvemento Comarcal de Galicia, Conselleria de Presidencia, Xunta de Galicia: Santiago de Compostela, Spain, 2001; pp. 173–218.
42. García-Rodeja, E.; Nóvoa-Muñoz, J.C.; Pontevedra-Pombal, X. Soils of Galicia. In *The Environment in Galicia: A Book of Images: Galician Environment Through Images*; Núñez-Delgado, A., Álvarez-Rodríguez, E., Fernández-Calviño, D., Eds.; Springer International Publishing: Cham, Switzerland, 2023; pp. 109–134. [CrossRef]
43. Goded, S.; Ekroos, J.; Domínguez, J.; Azcárate, J.G.; Guitián, J.A.; Smith, H.G. Effects of Eucalyptus Plantations on Avian and Herb Species Richness and Composition in North-West Spain. *Glob. Ecol. Conserv.* **2019**, *19*, e00690. [CrossRef]
44. Watson, D.F.; Philip, G.M. A Refinement of Inverse Distance Weighted Interpolation. *Geoprocessing* **1985**, *2*, 315–327.
45. Arnoldus, H.M.J. An Approximation of the Rainfall Factor in the Universal Soil Loss Equation. In *Assessment of Erosion*; De Boodt, M., Gabriels, D., Eds.; John Wiley and Sons: New York, NY, USA, 1980; pp. 127–132.
46. Instituto para la Conservación de la Naturaleza (ICONA). Mapas de Estados Erosivos. In *Cuenca Hidrográfica del Duero*; ICONA: Madrid, Spain, 1990; 96p.

47. Ministerio de Medio Ambiente. Inventario Nacional de Erosión de Suelos 2002–2012. In *Comunidad Autónoma de Galicia Pontevedra. 2003*; Ministerio de Medio Ambiente: Madrid, Spain, 2005; p. 206.
48. Moore, I.D.; Burch, G.J. Base física del factor longitud-pendiente en la ecuación universal de pérdida de suelo. *Soil Sci. Soc. Am. J.* **1986**, *50*, 1294–1298. [CrossRef]
49. Wischmeier, W.H. New developments in estimating water erosión. In Proceedings of the 29th Annual Meeting of the Soil Conservation Society of America, Ankeney, IA, USA, 4–6 May 1974; pp. 179–186.
50. Borrelli, P.; Märker, M.; Panagos, P.; Schütt, B. Modeling Soil Erosion and River Sediment Yield for an Intermountain Drainage Basin of the Central Apennines, Italy. *CATENA* **2014**, *114*, 45–58. [CrossRef]
51. Panagos, P.; Borrelli, P.; Meusburger, K.; Alewell, C.; Lugato, E.; Montanarella, L. Estimating the Soil Erosion Cover-Management Factor at the European Scale. *Land Use Policy* **2015**, *48*, 38–50. [CrossRef]
52. Hillel, D.; Warrick, A.W. *Environmental Soil Physics*; Nachdr. der Ausg. Edition 1998; AP Academic Press: Amsterdam, The Netherlands, 2009.
53. Rowell, D.L. *Soil Science: Methods & Applications*; Routledge: London, UK, 2014.
54. McCarty, L.B.; Hubbard, L.R.; Quisenberry, V.L. *Applied Soil Physical Properties, Drainage, and Irrigation Strategies*; Springer: Berlin/Heidelberg, Germany, 2016.
55. Panagos, P.; De Rosa, D.; Liakos, L.; Labouyrie, M.; Borrelli, P.; Ballabio, C. Soil Bulk Density Assessment in Europe. *Agric. Ecosyst. Environ.* **2024**, *364*, 108907. [CrossRef]
56. Lima, I.A.; Araújo, A.D.; Parteli, E.J.R.; Andrade, J.S.; Herrmann, H.J. Optimal Array of Sand Fences. *Sci. Rep.* **2017**, *7*, 45148. [CrossRef] [PubMed]
57. Itzkin, M.; Moore, L.J.; Ruggiero, P.; Hacker, S.D. The Effect of Sand Fencing on the Morphology of Natural Dune Systems. *Geomorphology* **2020**, *352*, 106995. [CrossRef]
58. Zainuddin, S.N.H.; Ariffin, E.H.; Taslin, P.N.A.; Dong, W.S.; Ramli, M.Z.; Abdul Maulud, K.N.; Awang, N.A.; Nadzri, M.I.; Ibrahim, M.S.I.; Ratnayake, A.S. Sand Dune Restoration as Sustainable Natural Architectural Design for Coastal Protection along Seasonal Storm-Prone Beach. *Results Eng.* **2024**, *22*, 102149. [CrossRef]
59. Zhao, H.L.; Zhou, R.L.; Su, Y.Z.; Zhang, H.; Zhao, L.Y.; Drake, S. Shrub Facilitation of Desert Land Restoration in the Horqin Sand Land of Inner Mongolia. *Ecol. Eng.* **2007**, *31*, 1–8. [CrossRef]
60. Stefanidis, S.; Alexandridis, V.; Ghosal, K. Assessment of Water-Induced Soil Erosion as a Threat to Natura 2000 Protected Areas in Crete Island, Greece. *Sustainability* **2022**, *14*, 2738. [CrossRef]
61. Piacentini, D.; Devoto, S.; Mantovani, M.; Pasuto, A.; Prampolini, M.; Soldati, M. Landslide Susceptibility Modeling Assisted by Persistent Scatterers Interferometry (PSI): An Example from the Northwestern Coast of Malta. *Nat. Hazards.* **2015**, *78*, 681–697. [CrossRef]
62. Mangor, K.; Drønen, N.K.; Kærgaard, K.H.; Kristensen, S.E. *Shoreline Management Guidelines*; DHI Water and Environment: Hørsholm, Denmark, 2017.
63. Arnáez, J.; Lana-Renault, N.; Lasanta, T.; Ruiz-Flaño, P.; Castroviejo, J. Effects of Farming Terraces on Hydrological and Geomorphological Processes. A Review. *CATENA* **2015**, *128*, 122–134. [CrossRef]
64. Merchán, L.; Martínez-Graña, A.; Nieto, C.E.; Criado, M.; Cabero, T. Geospatial Characterisation of Gravitational and Erosion Risks to Establish Conservation Practices in Vineyards in the Arribes Del Duero Natural Park (Spain). *Agronomy* **2023**, *13*, 2102. [CrossRef]
65. Prosdocimi, M.; Jordán, A.; Tarolli, P.; Keesstra, S.; Novara, A.; Cerdà, A. The Immediate Effectiveness of Barley Straw Mulch in Reducing Soil Erodibility and Surface Runoff Generation in Mediterranean Vineyards. *Sci. Total Environ.* **2016**, *547*, 323–330. [CrossRef]

Disclaimer/Publisher's Note: The statements, opinions and data contained in all publications are solely those of the individual author(s) and contributor(s) and not of MDPI and/or the editor(s). MDPI and/or the editor(s) disclaim responsibility for any injury to people or property resulting from any ideas, methods, instructions or products referred to in the content.